Analysis of Multistep Transformations in Single-Crystal NiTi

A.J. WAGONER JOHNSON, R.F. HAMILTON, H. SEHITOGLU, G. BIALLAS, H.J. MAIER, Y.I. CHUMLYAKOV, and H.S. WOO

The effects of composition and heat treatment on the thermally induced phase-transformation behavior of single-crystal NiTi with compositions of 50.1, 50.4, 50.8, and 51.5 at. pct Ni are presented in this article. Differential scanning calorimetry (DSC) experiments reveal that a heat-treated 50.1 at. pct Ni alloy exhibits an unprecedented multiple-step transformation (MST) on both heating and cooling, with up to four peaks. This behavior is absent in the higher-Ni-content alloys. In polycrystalline NiTi alloys, MSTs have been attributed to microstructure heterogeneities such as grain boundaries and dislocations, which influence precipitation. *In-situ* scanning electron microscopy (SEM) results show that the MST in the 50.1 at. pct Ni alloy is associated with single-crystal defects such as dendrites and low-angle boundaries. A heterogeneous precipitate distribution is observed in transmission electron microscopy (TEM) images of the same low-Ni alloy, also associated with the defects, creating conditions that have been shown in other studies to promote the MST in polycrystals. These MSTs are not observed for high-Ni single-crystal alloys containing the same defects. In this article, we describe the origin of the extraordinary forward and reverse MSTs in the low-Ni alloy and the absence of the MST in high-Ni alloys. Transformation sequences are proposed based on the contrasting precipitate microstructures.

I. INTRODUCTION

THE phase-transformation temperatures and sequence in near-equiatomic NiTi alloys are significantly influenced by alloy or matrix composition[1] and internal stresses in the matrix,[2] both of which can be altered by the precipitation of coherent Ti_3Ni_4 particles introduced under certain aging conditions.[3] Internal stresses can also be altered by the presence of defects such as dislocations introduced through mechanical deformation[2,4] or stress-free thermal cycling.[5]

Extensive information on transformation sequences in polycrystalline NiTi is reported in the literature using differential scanning calorimetry (DSC), but few studies have considered the phase-transformation behavior of single-crystal NiTi. The single-step forward (cooling) and reverse (heating) transformation sequence, austenite (A) $\leftrightarrow$ martensite (M), is typically observed in solutionized NiTi with little or no plastic deformation[6–11] or deformed then recrystallized NiTi.[1,12,13] Another sequence frequently reported is the two-step/two-step A $\leftrightarrow$ *R* $\leftrightarrow$ M transformation. The additional step is associated with the internal elastic stresses, which facilitate the transformation to the intermediate *R*-phase with a lower transformation shear.[2,4,5,8,10,13–15] The transformation sequences that are not as well described are those that include greater than two steps on cooling or heating. They are referred to here as multiple-step transformations (MSTs) and include sequences such as three-step/two-step and three-step/three-step transformations, for example.[15,16,17] In this study, we observe three-step/three-step and four-step/four-step transformations in single-crystal NiTi.

According to many studies on the MST in polycrystalline NiTi shape-memory alloys, the main considerations are microstructural heterogeneity and variations in local composition.[2,3,7,14–16] Microstructures containing precipitates are inherently heterogeneous, and some authors claim this as the source for MSTs.[15,17,18] In other cases, the MST is attributed to an inhomogeneous distribution of precipitates. High-angle grain boundaries[7,19] or dislocations[2,20] are cited as the most likely sources for inhomogeneous precipitation of Ti_3Ni_4 in polycrystals. In single crystals, these defects cannot be the source of inhomogeneous precipitation of Ti_3Ni_4. Grain boundaries are not present, nor are pre-existing dislocations after the long-term solutionizing heat treatment. Despite the lack of these particular sources for inhomogeneous precipitation, we are the first to report that single-crystal defects such as dendrites and low-angle boundaries do influence precipitation, particularly in the low-Ni-content alloys, and, thus, influence MST behavior. The MST is not observed in the higher-Ni-content single crystals that contain the same defects. To the contrary, the 50.8 and the 51.5 at. pct Ni alloys aged at 723 K for 1.5 hours exhibit a single forward phase transformation.

No rigorous investigation documenting MSTs on heating and cooling for single-crystal NiTi exists that reports on such a wide range of compositions and heat treatments. We investigate the phase-transformation behavior of single-crystal NiTi with compositions ranging from 50.1 to 51.5 at. pct Ni and for aging treatments from 0.5 to 100 hours at 723 K and for 1.5 hours at 823 K, respectively. This investigation of single crystals enhances the understanding of the origin of MSTs, since some of the explanations offered for the transformations do not apply to single crystals.[3,7,16] Specifically, our results show that low-Ni alloys have an extreme

A.J. WAGONER JOHNSON, Research Assistant Professor, H. SEHITOGLU, Professor, C.J. Gauthier Professor and Interim Head, and R.F. HAMILTON, Graduate Research Assistant, are with the Department of Mechanical Engineering, University of Illinois at Urbana–Champaign, Urbana, IL 61801. Contact e-mail: ajwj@uiuc.edu G. BIALLAS, Postdoctoral Associate, and H.J. MAIER, Professor, are with the Lehrstuhl für Werkstoffkunde (Materials Science), University of Paderborn, 33095 Paderborn, Germany. Y.I. CHUMLYAKOV, Professor, is with the Siberian Physical and Technical Institute, 634050 Tomsk, Russia. H.S. WOO, Professor, is with the Safety Engineering Department, Dongguk University, Sukjang-dong Kyongju Kyongbuk, South Korea.

Manuscript submitted February 24, 2004.

sensitivity to local composition, influenced by single-crystal defects, while high-Ni alloys do not. We focus our attention primarily on the origin of the MST on heating and cooling for the lowest-Ni-content alloys and explain its nonexistence in higher-Ni alloys. To characterize the phase transformations, we discuss the evolution of the DSC peaks with aging time. Finally, we explain the single peak observed for the highest-Ni alloys.

II. MATERIALS AND METHODS

A. *Single Crystals*

Bulk NiTi alloys with compositions of 50.1, 50.4, 50.8, and 51.5 at. pct Ni were supplied by Special Metals (New Hartford, NY). Alloys were fabricated using charge chemistry. The Bridgman technique was used to grow single crystals in graphite crucibles in an inert atmosphere. Ingots were subsequently homogenized in a vacuum furnace for 24 hours at 1193 K and then quenched.

B. *Heat Treatment and DSC*

Samples cut from the single-crystal ingots were encapsulated in vacuum and solutionized in an inert atmosphere for 2 hours at 1273 K. The aging treatments were conducted at 723 and 823 K for times ranging from 0.5 to 100 hours. All samples were water quenched. A Lindberg/blue-box furnace (BF51732 series) was used for heat treatments, and a Pyris 1 power-compensated differential scanning calorimeter (Perkin-Elmer Instruments) was used for the DSC experiments. The DSC samples weighing 20 mg were first heated to 100 °C to ensure an austenitic structure at the beginning of the experiment. Next, samples were cooled continuously to −100 °C, heated to 100 °C, and, finally, cooled to room temperature. The heating/cooling rate during the entire experiment was 10 °C/min. The low-temperature capability for the calorimeter used in this study is −150 °C.

C. *Transmission Electron Microscopy*

A low-speed diamond saw was used to section the single crystals for transmission electron microscopy (TEM) samples. Thin sections were mechanically ground to a thickness of 150 μm and then polished. Electron transparency was obtained by conventional twin-jet polishing using a 5 pct perchloric acid and 95 pct ethanol solution. The typical polishing temperature was −15 °C. Note that this temperature is below the martensite start temperature for the near-equiatomic NiTi alloys. Therefore, martensite may form during electropolishing in samples with the lowest Ni content. In these cases, either polishing conditions were adjusted, or an appropriate heat treatment was employed during TEM to eliminate such artifacts. The double-tilt holder used in this study allowed for moderate heating of the TEM foil up to 100 °C, which is well above the austenite finish temperature.

D. *Scanning Electron Microscopy*

The sample surface for both the conventional scanning electron microscopy (SEM) imaging and the heating/cooling experiments was electropolished using the same procedure as described earlier for TEM sample preparation. Small changes in orientation resulting from the underlying dendritic microstructure were detected using a channeling contrast technique, which requires backscattered electron (BSE) imaging. Conventional secondary electron (SE) contrast was used to image the small change in surface topography associated with the phase transformations. For the heating/cooling experiments, the sample was placed on a three-stage Peltier element, and the specimen temperature was measured using miniature thermocouples pressed onto the sample. Temperature gradients were minimized by using a 1-mm-thick sample. The vacuum environment inherent to the SEM helped to reduce temperature gradients even further. The sample was first heated to 60 °C, which ensured a fully austenitic structure at the beginning of the experiment. Next, the sample was cooled from 60 °C to −60 °C at 10 °C increments. The transformation was observed and recorded at each temperature increment.

III. EXPERIMENTAL RESULTS

A. *Differential Scanning Calorimetry*

The 50.1 at. pct Ni alloy exhibits particularly unique behavior; MSTs with up to four peaks are observed on both heating and cooling and for aging times ranging from 1.5 to 100 hours. Figure 1 shows the normalized DSC results for the 50.1 at. pct Ni alloy heat treated at 723 K. First, consider the data on cooling. The solutionized alloy exhibits a

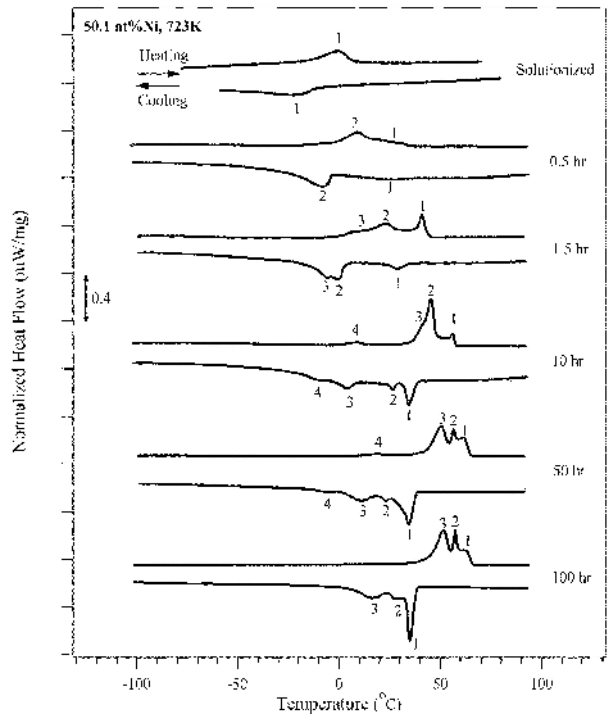

Fig. 1—Normalized DSC curves for the 50.1 at. pct Ni alloy heat treated at 723 K for 0, 0.5, 1.5, 10, 50, and 100 h. Each numbered peak represents a phase transformation. Of special note are the numbers of peaks and their evolution on cooling for heat treatments greater than 0.5 h and that the peak behavior is equivalent for the reverse transformation.

single peak. A relatively small peak typically associated with the *R*-phase transformation, peak 1 (P1), is present after 0.5 hours of aging and shifts to a higher temperature relative to the solutionized case. Three and four peaks are present at 1.5 and 10 hours of aging, respectively, which reveal the initiation and evolution of the MST. The three-step/three-step and, in particular, the four-step/four-step transformation sequences for the MSTs are not as well documented. Here, we point out significant features of the MSTs observed in these DSC results. The data on cooling for 50 hours are similar to those for 10 hours, except that the magnitude of peak P4 decreases for the longer heat treatment. At 100 hours, peak P1 is larger than for any other heat treatment and P4 no longer exists. When heated, the reverse transformation occurs in one step in the solutionized state. The heating curve for the 0.5-hour heat treatment contains two rather broad and overlapping peaks, P1 and P2. The number of peaks increases to three at 1.5 hours and to four at 10 and 50 hours of heat treatment. At 100 hours, only three peaks remain. As with cooling, peak P4 decreases in magnitude between 10 and 50 hours of heat treatment, as seen in Figure 1, until it is no longer detected at 100 hours. Peak 3 grows between 10 and 100 hours, while the magnitude of P1 remains fairly constant. Peak 2 decreases in magnitude between 10 and 50 hours, but does not change significantly after 50 hours. The transformation sequences on heating and cooling are proposed in the discussion.

Figure 2 summarizes the change in the transformation (or peak) temperature associated with each transformation and aids in understanding the evolution of the MST and in the discussion of the transformation sequences. In the text, each transformation that evolves with time is referred to by the number of the last peak on the corresponding curve in Figure 2. In the forward transformation, in Figure 2(a), the temperatures for both transformations 1 and 3 increase with increasing aging time, while those for transformations 2 and 4 remain constant by comparison, changing less than 2 °C overall. The peak temperatures for transformation 1 increase approximately 10 °C from 0.5 to 10 hours and then remain fairly constant. The most significant increase in temperature is for transformation 3, which increases by 24 °C between 0.5 and 100 hours of aging. In the reverse transformation, in Figure 2(b), the temperatures associated with transformations 1 through 3 increase significantly with time at similar rates, but tend toward a steady state by 100 hours. Even though there are contrasts in the evolution of the reverse and forward transformation temperatures, we still observe equivalent numbers of heating and cooling peaks for each heat treatment.

The DSC behavior described in detail previously for the 50.1 at. pct Ni can be contrasted with that of the 50.4, 50.8, and the 51.5 at. pct Ni alloys in Figures 3(a) and (b), which show the DSC results for the 1.5-hour heat treatment at 723 and 823 K, respectively. The most interesting observation is that the MST is absent in higher-Ni-content alloys at either heat-treatment temperature. Furthermore, the DSC results for 50.8 and 51.5 at. pct Ni show only one peak on cooling and one broad peak on heating for the heat treatment at 723 K, while two are present on cooling and one on heating at 823 K. At 723 K, the intermediate composition studied (50.4 at. pct Ni) exhibits two distinct peaks on cooling and one peak on heating. At 823 K, in Figure 3(b), the same alloy shows two peaks, possibly three, on cooling, and two overlapping peaks on heating. This may be interpreted as a MST and is considered a borderline case.

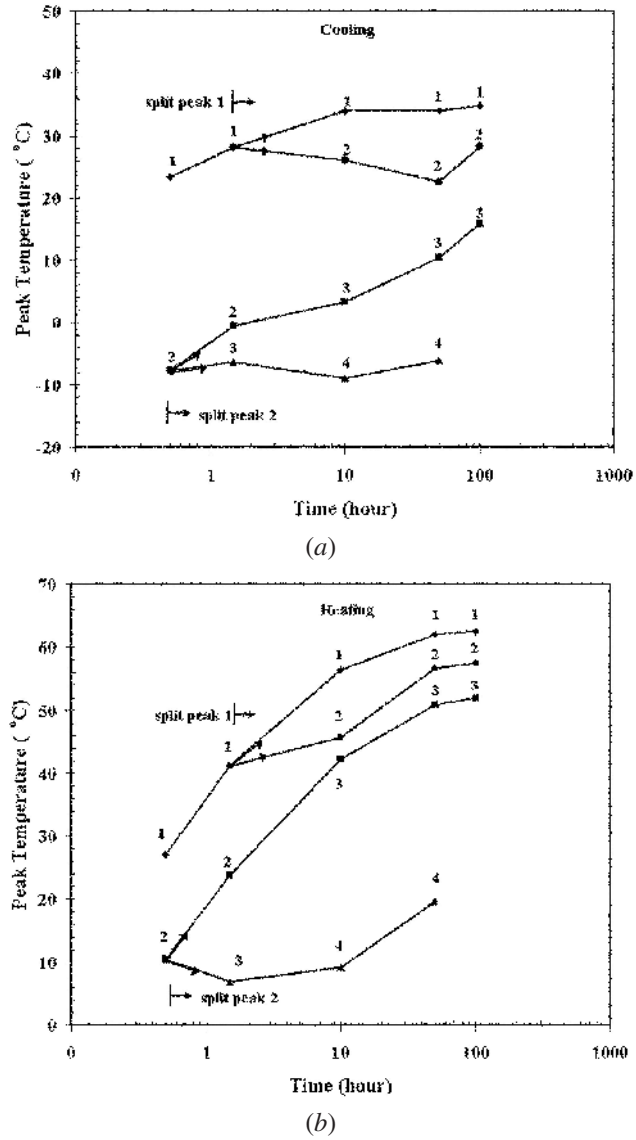

Fig. 2—Peak evolution for transformations 1 through 4 for the 50.1 at. pct Ni alloy heat treated at 723 K. Data points are numbered according to the peak-labeling convention used in Fig. 1. Arrows indicate splitting of a peak. Evolution (*a*) for cooling and (*b*) for heating.

B. *Transmission Electron Microscopy*

Figures 4(a) and (b) are TEM images of the 50.1 and the 51.5 at. pct Ni alloys aged at 823 K for 1.5 hours. These figures qualitatively show the distinct difference in the spacing and volume fraction of precipitates between the alloys with the highest and lowest Ni contents. Figures 5(a) and (b) compare the size and spacing of precipitates in the 50.8 at. pct Ni alloy heat treated for 1.5 hours at 723 and 823 K, respectively. The sample aged at 823 K clearly shows that precipitates coarsen significantly at the higher aging temperature for the same aging time. Furthermore, the dark contrast induced by the stress fields surrounding the coherent

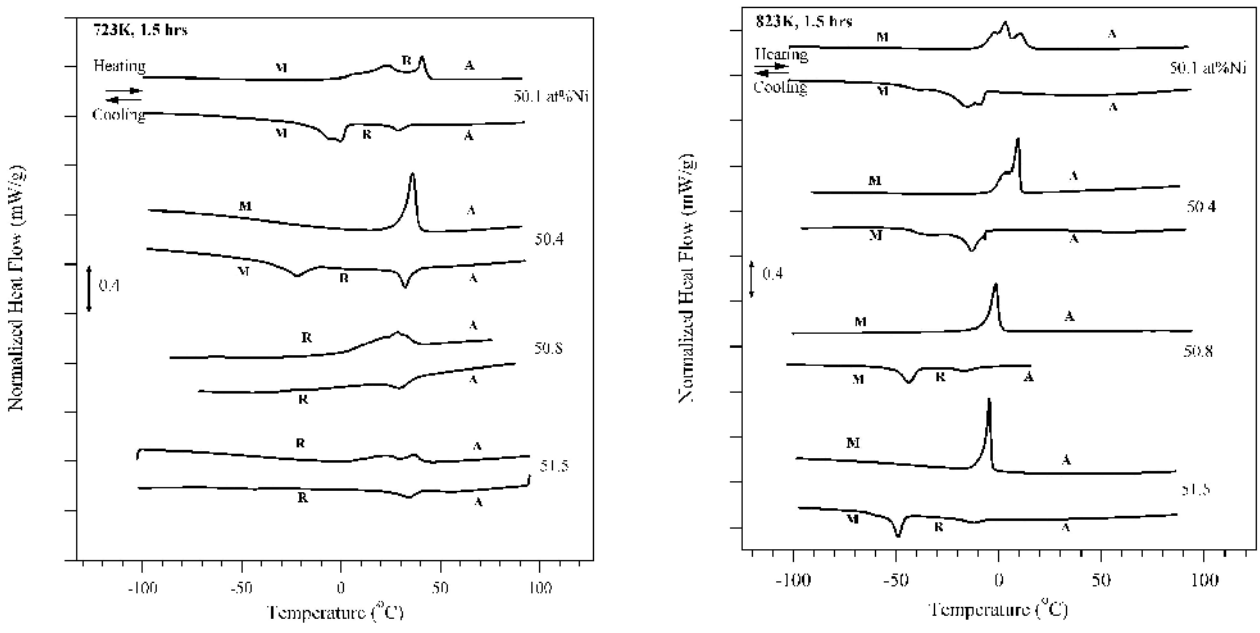

Fig. 3—The DSC curves for the 50.1, 50.4, 50.8, and 51.5 at. pct Ni alloys. Samples aged for 1.5 h at (*a*) 723 K and (*b*) 823 K. Note the multiple peaks in the 50.1 at. pct Ni curves and the single peaks in the 50.8 and 51.5 at. pct Ni alloys.

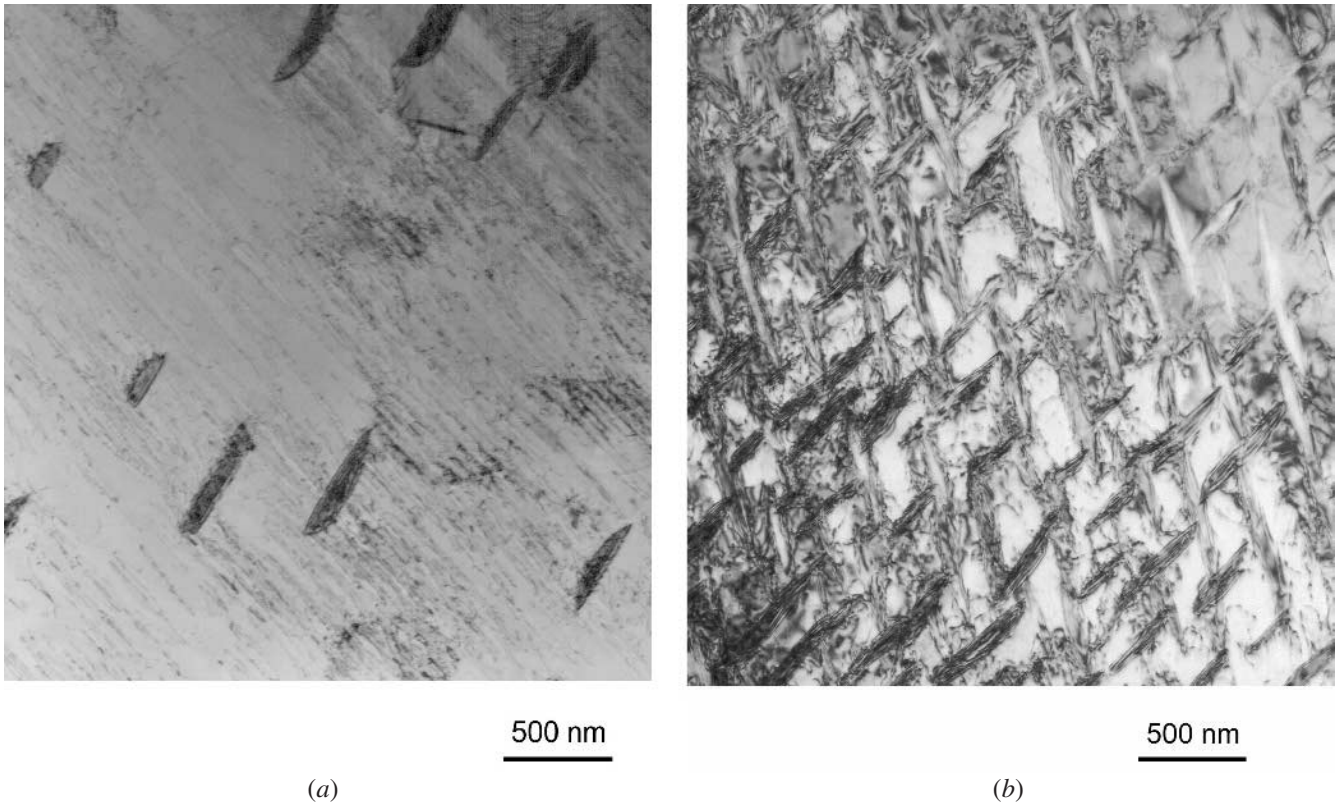

Fig. 4—Samples aged 1.5 h at 823 K, showing relative precipitate size, spacing, and distribution: (*a*) 50.1 at. pct Ni[26] and (*b*) 51.5 at. pct Ni.

precipitates in Figure 5(a) is not as prominent in Figure 5(b). Note that the sample used in Figure 4(b) was imaged after a series of straining experiments and, thus, the dislocation density is significantly higher than in the actual virgin samples used for DSC. However, this is irrelevant for the purpose of showing relative precipitate fractions and spacings.

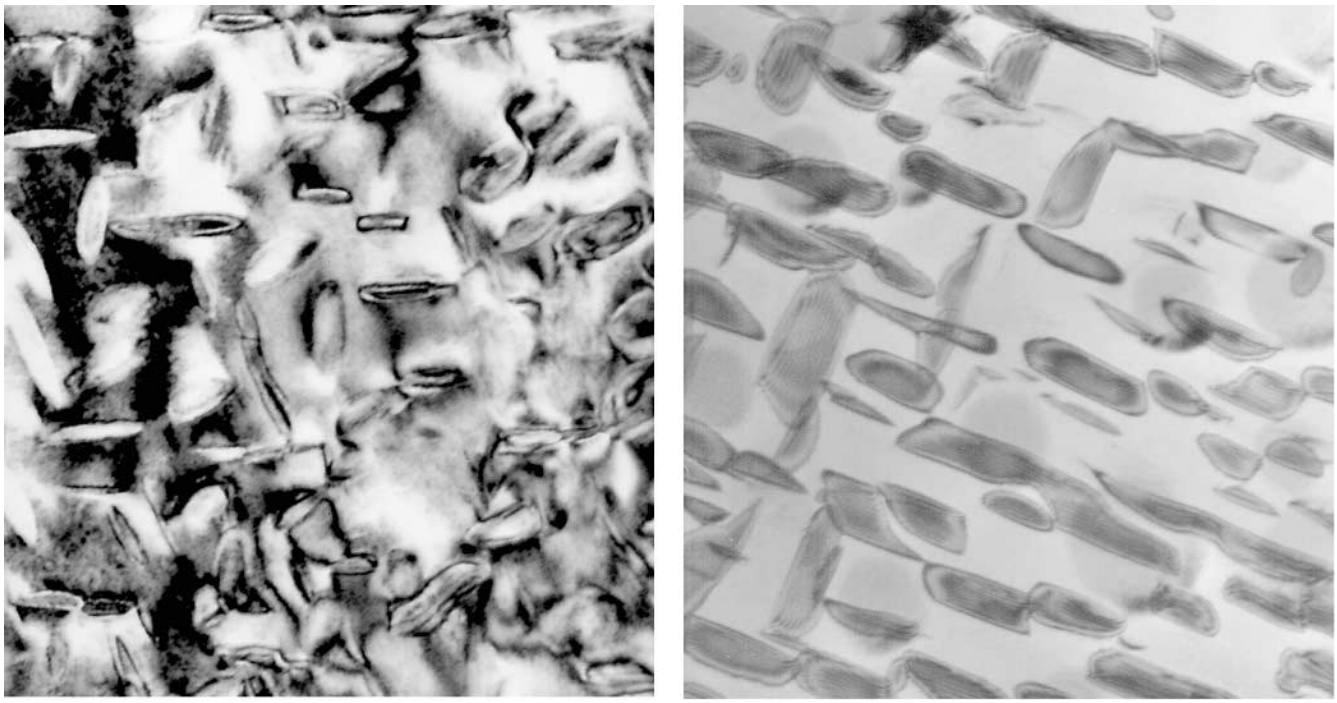

(*a*) (*b*)

Fig. 5—The TEM images of 50.8 at. pct Ni aged for 1.5 h at (*a*) 723 K and (*b*) 823 K, showing the relative precipitate spacing and size.

C. *Scanning Electron Microscopy*

The SEM was used to highlight the "defects" present in the single crystals on a length scale larger than is possible using TEM. While the other alloys contain similar defects, the behavior of the 50.1 at. pct Ni alloy is affected much more significantly. The results are highlighted in Figures 6 through 8. Figure 6 is a BSE image of an array of low-angle tilt boundaries in the 50.1 at. pct Ni alloy. The boundaries are aligned from the upper-right to the lower-left of the image and are emphasized with arrows. An insignificant volume fraction of TiC particles and some pores, which are inherent to growing single crystals in graphite crucibles and to casting, respectively, decorate the boundaries. We emphasize that these defects are also observed in the other NiTi alloys studied. Figures 7(a) and (b) are images formed in SE mode to emphasize surface topography induced by the martensitic transformation at the thermocouple readings of −50 °C and −60 °C, respectively. At −50 °C, few martensite plates are visible in region A and markedly fewer are visible in region B, as compared to region A. As the temperature decreases to −60 °C, martensite is present in almost all regions of the image, but predominantly in region A. Evidence of self-accommodating martensite (SAM) is indicated with triangles in Figure 7, and SAM forms in regions unaffected by precipitates. Following the cooling experiment, the sample was imaged again using the BSE technique, because imaging both the tilt boundaries associated with the compositional variation and the inhomogeneous martensitic transformation simultaneously is not possible. The amount of contrast introduced by the tilt boundary would no longer be visible once an appreciable amount of martensite forms. The sample was first heated to 80 °C to ensure transformation back to the B2 structure and was then cooled to room temperature. These results are shown in Figure 8(a). The image clearly shows the presence of the tilt boundaries, which can be seen as roughly parallel, diagonal lines across the image. Residual martensite is also present. The tilt boundaries and residual martensite are depicted schematically in Figure 8(b).

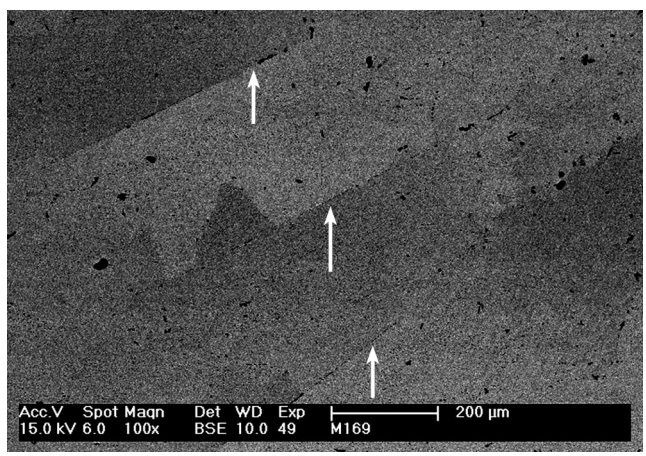

Fig. 6—Region of 50.1 at. pct Ni, showing several low-angle tilt boundaries aligned from the bottom-left to the top-right of the image (shown by arrows). The sample was imaged using backscattered electrons.

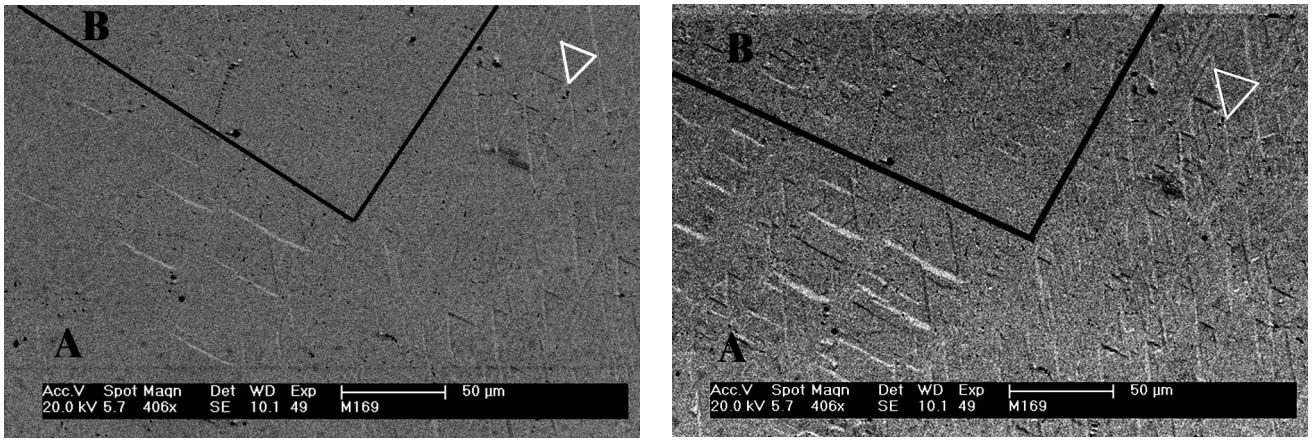

(*a*) (*b*)

Fig. 7—Secondary electron images from the heating/cooling experiment conducted on the 50.1 at. pct Ni alloy. Sample images at (*a*) −50 °C and (*b*) −60 °C. Note that there are remarkably fewer martensite plates present in region B of (a). Evidence of self-accommodating martensite is shown using white triangles in (a) and (b).

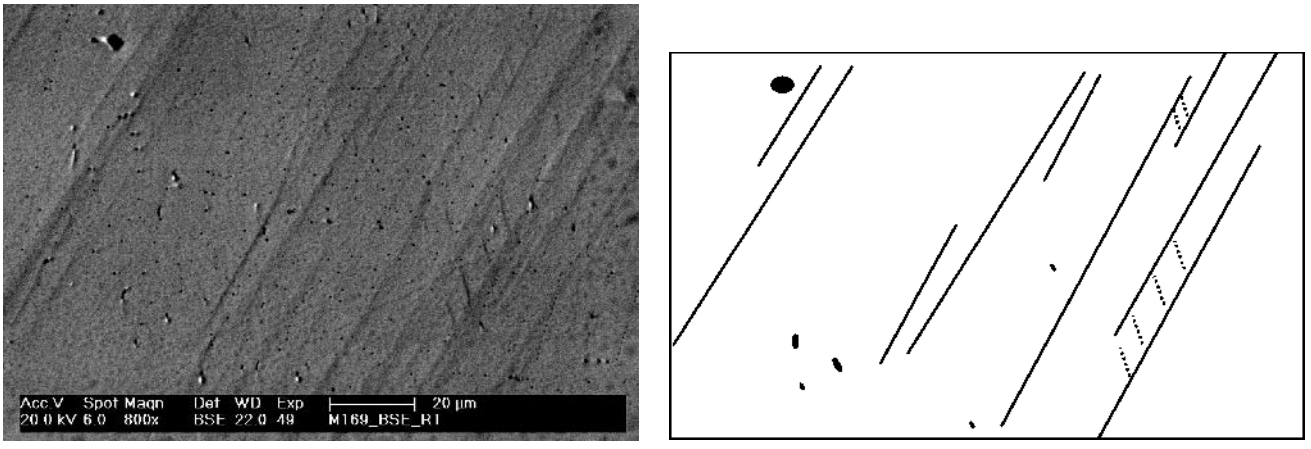

(*a*) (*b*)

Fig. 8—(*a*) The BSE image of the 50.1 at. pct Ni alloy, showing a region from Figure 7 after the heating/cooling experiment. The bands are low-angle tilt boundaries, and residual martensite can be seen. (*b*) Schematic of bands, several voids, and residual martensite. The martensite and low-angle boundaries are represented by dashed and solid black lines, respectively.

IV. DISCUSSION OF CONTRAST IN TRANSFORMATION SEQUENCES FOR LOW- AND HIGH-NI ALLOYS

Because these alloys are undeformed single crystals, there are no grain boundaries and the dislocation density in virgin samples is low.[8] Therefore, one would not expect to observe a MST in single crystals. Accordingly, MSTs are not observed in the higher-Ni single-crystal alloys. The 50.1 at. pct Ni single crystal, on the other hand, exhibits unparalleled MST behavior that suggests an extreme sensitivity of low-Ni-content alloys to small variations in local composition and precipitate arrangement. In this section, we explain how variations in local composition generate MSTs in 50.1 at. pct Ni. We then propose the transformation sequences for the forward and reverse transformations based on DSC data and SEM results. Finally, the lack of MSTs in alloys with a high Ni content, containing the same defects, is explained, and the DSC behavior is contrasted with that of the 50.1 at. pct Ni alloy.

A. *Origin of MSTs in the 50.1 at. pct Ni Alloy*

Dendrites are a type of defect present in single crystals that form during solidification, and these defects are often associated with compositional variations in other materials such as in Ni-based superalloys.[21] Also fairly common in single crystals, and associated with the dendrites, is the low-angle tilt boundary.[22] Figures 6, 7 and 8 confirm the presence of these two types of defects in the 50.1 at. pct Ni alloy and show that they correspond to local variations in phase-transformation behavior.

The compositional variations resulting from the formation of dendrites and low-angle boundaries produce an inhomogeneous precipitate distribution that promotes MST on both heating and cooling. This is the central theme for the cause of MST in the 50.1 at. pct Ni. More specifically, the local variations in Ni content result in a composite of regions with less than region I and greater than region II_p (50.1 at. pct Ni). NiTi alloys with greater than 50.0 at. pct Ni precipitate Ti_3Ni_4 during heat treatment. Because the 50.1 at. pct

Table I. Summary of Transformations (Forward) and Corresponding Peaks for 50.1 At. Pct Ni Solutionized and Aged between 0.5 to 100 Hours at 723 K

Peak	Solutionized	0.5 h	1.5 h	10 h	50 h	100 h
1	$(A \rightarrow M)_{I,IIp}$	$(A \rightarrow R)_{IIp}$ $(R \rightarrow M)_{IIp}$	$(A \rightarrow R)_{IIp}$ $(R \rightarrow M)_{IIp}$	$(A \rightarrow R)_{IIp}$ $(R \rightarrow M)_{IIp}$	$(A \rightarrow R)_{IIp}$ $(R \rightarrow M)_{IIp}$	$(A \rightarrow R)_{IIp}$ $(R \rightarrow M)_{IIp}$
2		$(A \rightarrow M)_{IIp}$ $(A \rightarrow M)_{I}$	$(A \rightarrow M)_{IIp}$	$(R \rightarrow M)_{IIp}$	$(R \rightarrow M)_{IIp}$	$(R \rightarrow M)_{IIp}$
3			$(A \rightarrow M)_{I}$	$(A \rightarrow M)_{IIp}$	$(A \rightarrow M)_{IIp}$	$(A \rightarrow M)_{I,IIp}$
4				$(A \rightarrow M)_{I}$	$(A \rightarrow M)_{I}$	

I, II_p: Regions I and II_p not containing and containing precipitates, respectively.

Ni has an inherently low volume fraction of precipitates, it is likely that precipitates do not form in an appreciable amount in region I. Therefore the dominant transformation is $(A \leftrightarrow M)$, and this will be denoted $(A \leftrightarrow M)_I$; region I behaves more like a solutionized alloy. Precipitates do form in region II_p in some fraction; region II_p behaves like an aged alloy. The relative volume fractions of regions I and II_p were not determined for this discussion. It is important to note that these defects and compositional variations must also be present in the aged higher-Ni-content single crystals and the NiTi alloys in the solutionized state. A solutionized alloy does not contain precipitates. Consequently, a MST does not occur. The lack of a MST in aged alloys is discussed in Section IV-C.

B. *Transformation Sequences for Aged, Single-Crystal 50.1 at. pct Ni*

The data in Figures 1 and 2 clearly show that there is a marked difference in the transformation behavior of the 50.1 at. pct NiTi on cooling (heating discussion at the end of this section, Section IV-B) as compared to the higher-Ni alloys or polycrystalline NiTi. Furthermore, the unusual MST at 10 hours and greater has not been observed previously. A discussion of logical possibilities for the transformations observed follows, and Table I summarizes the transformation sequences proposed for the 50.1 at. pct Ni alloy on cooling. First consider the $A \rightarrow M$ transformation. In the solutionized case, the broad peak for $A \rightarrow M$ suggests that the transformation peaks for regions I and II_p overlap, such that they cannot be distinguished. After 0.5 hours of aging, the first and very small peak, P1, is related to the R-phase formation in the vicinity of precipitates in region II_p. The associated heat of transformation suggests that only a very small fraction of R-phase forms for this aging condition. Transformation peaks at 0.5 hours for $A \rightarrow M$ in regions I and II_p occur at peak P2. The temperature of P2 has increased due to the Ni depletion in region II_p caused by precipitation of Ti_3Ni_4.

Figures 9(a) and (b) are schematics of the SEM and TEM images in Figures 6 and 4(a), respectively, which can be used to illustrate the transformations in regions I and II_p. Figure 9(a) depicts the low-angle boundary separating the two regions, and Figure 9(b) shows a high-magnification schematic of region II_p, with the R-phase surrounding each precipitate (solid lines) and the $(A \rightarrow M)_{IIp}$ transformation taking place away from the precipitates. With increasing aging time, the Ni-rich precipitates coarsen in region II_p, and the Ni concentration in the matrix continues to decrease. Beginning at 1.5 hours of aging, the $A \rightarrow M$ transformations in regions

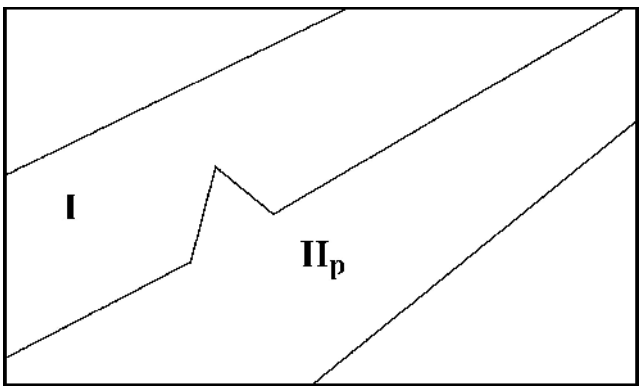

(*a*)

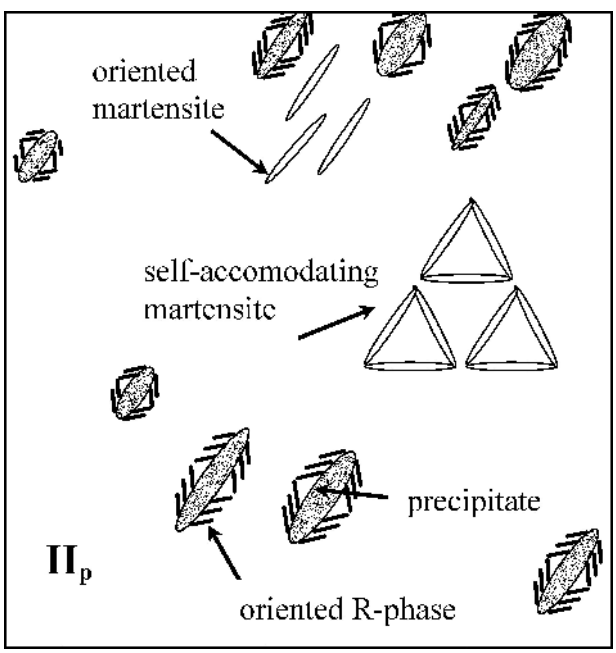

(*b*)

Fig. 9—Schematic depicting the inhomogeneous precipitation of Ti_3Ni_4 and transformation of martensite. (*a*) Schematic of the SEM image in Fig. 6, showing low-angle boundaries separating region I, without precipitates, and region II_p, containing precipitates. (*b*) Schematic of the TEM image in Fig. 4(a) showing oriented *R*-phase (solid black lines) near precipitates (gray ovals), oriented martensite (aligned laths), and self-accomodating martensite (laths grouped by three) away from precipitates.

I and II_p are distinguishable on the DSC curve in Figure 1 as peaks P2 (II_p) and P3 (I). For 10 hours, peaks P2 and P3 at 1.5 hours are associated with transformations 3 and 4,

respectively, as is shown in Figure 2. The increase in transformation temperature for transformation 3 can be associated with two factors, namely, the Ni depletion of the matrix[8] and the resulting decrease in yield strength of the matrix. According to Hornbogen,[23] the martensite start temperature (M_s) varies with aging time (t) according to Eq. [1]:

$$\frac{dM_s}{dt} = \frac{\delta T_o}{\delta c}\frac{\delta c}{\delta t} - \frac{\delta \Delta T}{\delta \tau_y}\frac{\delta \tau_y}{\delta t} \qquad [1]$$

where T_o is the equilibrium transformation temperature for a given composition, c is the concentration of Ni in the matrix, ΔT is the undercooling required to complete the transformation, and τ_y is the yield strength of the matrix. For NiTi, $\delta T_o/\delta c$ is negative and $\delta c/\delta t$ is negative or zero, depending on whether precipitation is ongoing or complete (*i.e.*, the matrix is 50.0 at. pct Ni). Therefore, the first term is positive or zero. The term $\delta \Delta T/\delta \tau_y$ is always positive, as the undercooling increases with yield strength.[23] Finally, the term $\delta \tau_y/\delta t$ is negative at almost all aging times in the 50.1 at. pct Ni alloy; the volume fraction of coherent or semicoherent precipitates is so low that their stress fields cannot increase the matrix strength, but the Ni depletion does decrease the yield strength of the matrix. This combination of properties with aging time leads to the observed increase $\left(\frac{dM_s}{dt} > 0\right)$ in the $(A \rightarrow M)_{II_p}$, peak P3, temperature with aging time.

It is possible that by 100 hours, the composition of the matrix including regions I and II_p is homogeneous and approaches the composition of region II_p. More specifically, after 100 hours of heat treatment, P3 represents the $A \rightarrow M$ transformation for the portion of the matrix in regions I and II_p unaffected by precipitates, with a composition equal to 50.0 at. pct Ni. This is supported by the experimental observation that the heat of transformation associated with transformation 4 decreases in magnitude, while that of transformation 3 increases, which also suggests a decrease in the volume of material with the composition of region I and an increase in volume of material with the composition of region II_p.

In order to rationalize the remaining peaks, we refer to results from two independent *in-situ* investigations of the MST in polycrystalline NiTi using either TEM or neutron diffraction. Bataillard *et al*. observed four distinct transformations in an aged (793 K for 30 minutes) 51.14 at. pct Ni alloy using TEM, but only three peaks appeared on the DSC curve.[15] We remark that Bataillard *et al*. are the only ones to observe this sequence using *in-situ* TEM. Sitepu *et al*. used neutron diffraction to determine phase fractions present during heating and cooling experiments.[18] They examined an aged (673 K for 20 hours) 50.7 at. pct Ni alloy. Two peaks were present on the DSC cooling curve. Their diffraction results showed that both the R-phase and the B19' martensite were present at temperatures between the first and second peaks. The TEM images supported the neutron-diffraction results. Results by Bataillard *et al*. and Sitepu *et al*. demonstrate that two different phase transformations can occur within the same thermal event recorded in the DSC experiment. We believe that an *in-situ* measurement, such as neutron diffraction, would be necessary in order to provide with absolute certainty the exact transformation sequence for this 50.1 at. pct Ni single-crystal alloy. This type of experiment is out of the scope of this article, but we use their results to interpret our results.

The relative magnitude of peak P1 at 10, 50, and 100 hours of aging, as compared to peak P1 at 0.5 and 1.5 hours and other peaks not associated with transformation 1, is indicative of a greater fraction of R-phase and perhaps another phase transformation occurring within that peak for the longer aging times. The R-phase has been observed to nucleate from dislocations in the matrix.[24] Therefore, punched-out dislocations, as the matrix softens and as precipitates coarsen and lose coherency, may provide another nucleation source for the R-phase in addition to Ti_3Ni_4 precipitates. The punched-out dislocations would affect primarily region II_p, since the low-angle tilt boundaries separating regions I and II_p would impede their motion under a stress-free thermal cycle. If the density of punched-out dislocations increases with aging time, the total heat of transformation of $A \rightarrow R$ for peak P1 between 10 and 100 hours would increase. The work by Sitepu *et al*. provides support that the $R \rightarrow M$ transformation could also take place within peak P1 at 10, 50, and 100 hours of aging.[18] The second peak, which is small by comparison, would include the $R \rightarrow M$ transformation for any remaining R-phase within region II_p affected by precipitate-stress fields and punched-out dislocations. The unaffected regions within region II_p would transform from austenite to martensite along with region I, as mentioned earlier.

The number of thermal events observed on heating for the 50.1 at. pct Ni alloy is the same as that observed on cooling, suggesting that the inhomogeneous microstructure strongly affects the behavior on the reverse cycle as well. Most studies have shown or have assumed that the exact reverse of the cooling transformation occurs on heating. Based on the results presented in Figures 1 and 2, which show the peak evolution with time and the corresponding positive peak-to-peak hysteresis, this seems to be a reasonable assumption.

C. *The DSC Behavior and Lack of MST in High-Ni Single Crystals*

The higher-Ni alloys in this study do not exhibit a MST. Both Bataillard *et al*. and Dlouhy *et al*. reported a MST in polycrystalline 51.14 and 50.7 at. pct Ni, respectively, for aging conditions similar to those considered in this study.[15,19] Without the MST data from the single-crystal 50.1 at. pct Ni alloy, one might argue that the lack of a MST is simply because of the single-crystal samples being studied. However, the same single-crystal defects visible using SEM that are attributed to MST in the 50.1 at. pct Ni alloy are also present in the higher-Ni single-crystal alloys. In contrast to the 50.1 at. pct Ni, TEM results show that with a higher Ni concentration, the alloys have a significantly more homogeneous precipitate arrangement, thus eliminating the conditions that promote MST. The homogeneous precipitate distribution can be explained as follows. In the single crystals, some regions contain more and some less than the nominal composition of the alloy. For 50.1 at. pct Ni, this implies that one region must be near-equiatomic and, under such conditions, no precipitates form. For the higher-Ni alloys, the compositions in the low-Ni and high-Ni regions of the sample contain enough Ni to form a significant volume of precipitates in all regions of the sample. The borderline case may be for the 50.4 at. pct Ni, which shows some evidence of sensitivity to these defects and variations in local compo-

sition. The results clearly demonstrate that precipitate distribution dictates the conditions for MST.

Not only do the 50.8 and the 51.5 at. pct Ni alloys lack a MST, they also show only one peak in the DSC data for the 723 K heat treatment on cooling. Two are present at 823 K. The contrasting behavior for the two heat treatments is now explained, beginning with a discussion of the R-phase transformation and ending with the suppression of the R → M transformation at 723 K. The first peak (the only peak at 723 K) is associated with the A → R transformation, and the transformation temperature does not show a strong dependence on Ni content. The result is consistent with previous results by Somsen *et al*., who showed that the A → R transformation temperature is constant as a function of composition at 723 K in polycrystalline NiTi.[25] The transformation strain for A → R is an order of magnitude less than that for A → M; the latter transformation is highly sensitive to stress fields introduced by defects such as coherent precipitates, while the former is not.[26] Consequently, the precipitate arrangement resulting from the nominal alloy composition should not significantly influence the A → R transformation temperature. The same result was observed at 823 K.

In contrast to the MST in lower-Ni alloys, the second peak expected for aged NiTi alloys (R → M) is suppressed below the detection capabilities of DSC for the 50.5 and 51.5 at. pct Ni alloys. In the absence of polycrystalline defects, our results indicate that two factors are likely to contribute. The first is that the precipitate spacing may be smaller than the critical nucleus size; therefore, the martensite nucleation is suppressed. The second is that a larger undercooling is required in the presence of the high strain energy associated with the large volume fraction of closely spaced, coherent precipitates. The latter can be argued thermodynamically using Eq. [1]. For the R → M transformation to be suppressed, the term $\frac{\delta \Delta T}{\delta \tau_y} \frac{\delta \tau_y}{\delta T}$ must be large and positive. This is possible if the strain fields associated with the coherent particles more than compensate for the decrease in yield strength caused by the Ni depletion. Note that the aging time from Eq. [1] is interchangeable with temperature.

One peak is observed on heating for both heat-treatment temperatures. For the heat treatment at 723 K, the M → R transformation is suppressed. Therefore, we attribute the apparently broad, overlapping heating peaks to concomitant R → A transformations in regions with and without the aforementioned single-crystal defects. At 823 K, the single peak rises steeply on the back side (higher temperature), but is less steep on the front side (lower temperature). This may be an indication that the M → R and R → A transformations overlap. The possibility of overlapping heating peaks suggests that the high-Ni alloys exhibit some sensitivity to microstructure heterogeneity even though the MST is absent.

V. CONCLUSIONS

In this study, we examined the origin of the MSTs on heating and cooling in single-crystal NiTi shape-memory alloys. The work provides valuable insight into the influence of local composition on the MST and confirms that the resulting inhomogeneous precipitation plays a dominant role in the MST. We report the following findings.

1. The MST in 50.1 at. pct Ni with up to four peaks on heating and cooling results from the precipitate arrangement following aging. The inhomogeneous distribution of precipitates is caused by small compositional variations in the single crystal that are attributed to dendrites and low-angle subgrain boundaries and results in regions without precipitates (region I) and regions with precipitates (region II_p). These two regions, therefore, show different phase-transformation behaviors, which manifests itself as multiple peaks on the DSC curves even at heat treatments as long as 100 hours. The cause of the MST for single crystals, namely the inhomogeneous precipitate microstructure, is equivalent to some reports for polycrystals. The source for inhomogeneous precipitation in single crystals is different than that for polycrystals.
2. The proposed transformation sequence for the MST in the 50.1 at. pct Ni alloy is summarized in Table I. The peak evolution on cooling supports that the last peak in the sequence is the austenite-to-martensite transformation in regions I (without precipitates) and II_p (with precipitates). The evolution of the first peak on cooling indicates that, in addition to the austenite to R-phase transformation, another transformation such as the R-phase–to–martensite transformation takes place. Our findings provide experimental evidence to substantiate that when the MST is observed, the reverse transformation corresponds exactly to that of the forward transformation.
3. The high-Ni-content alloys do not exhibit MST, but do contain the same defects. The TEM confirms a homogeneous precipitate arrangement. Therefore, we conclude that the nominal Ni content is sufficiently greater than 50.0 at. pct Ni, such that precipitates form in all regions of the sample. In the absence of polycrystalline defects such as grain boundaries, the homogeneity of the precipitates suppresses MST. There is some evidence that there may be sensitivity to the MST, especially for the intermediate (50.4 at. pct Ni) case.
4. A large undercooling is necessary for the martensitic transformation at 723 K for the 50.8 and 51.5 at. pct Ni single-crystal alloys. The precipitate spacing and the strain energy associated with their coherency and spacing are likely to suppress the R-*phase*–to-martensite transformation to temperatures below the measuring capabilities of the DSC equipment used in the study.

ACKNOWLEDGMENTS

One of the authors (HS) acknowledges the partial support of AFSOR, Aerospace and Materials Sciences, and the National Science Foundation (Grant No. CMS-0428428). HJM was supported by Deutsche Forschungsgemeinschaft.

REFERENCES

1. A. Goyobu, Y. Kawamura, H. Horikawa, and T. Saburi: *Mater. Trans. JIM*, 1996, vol. 37, pp. 697-702.
2. D. Treppmann and E. Hornbogen: *J. Phys. IV*, 1995, vol. 5, pp. 211-16.
3. L. Bataillard and R. Gotthardt: *J. Phys. IV*, 1995, vol. 5, pp. 647-52.
4. D. Chrobak and H. Morawiec: *Scripta Mater*., 2001, vol. 44, pp. 725-30.
5. T. Tadaki, Y. Nakata, and K. Shumizu: *Trans. Jpn. Inst. Met*., 1987, vol. 28, pp. 883-90.
6. H. Sehitoglu, R. Hamilton, H.J. Maier, A. Wagoner Johnson, H. Woo, and Y. Chumlyakov: "Detwinning and Hysteresis in NiTi Alloys,"

Proceedings from New Trends in Phase Transformation and their Applications to Smart Structures, NATO International Workshop Metz, France April 23-26, 2002.
7. J. Khalil-Allafi, A. Dlouhy, and G. Eggeler: *Acta Mater.*, 2002, vol. 50, pp. 4255-74.
8. K. Gall, H. Sehitoglu, Y. Chumlyakov, I.V. Kireeva, and H.J. Maier: *Trans. ASME, JEMT*, 1999, vol. 121, pp. 28-37.
9. K. Gall, H. Sehitoglu, Y.I. Chumlyakov, and I.V. Kireeva: *Acta Mater.*, 1999, vol. 47, pp. 1203-17.
10. K. Gall, H. Sehitoglu, Y.I. Chumlyakov, Y.L. Zuev, and I. Karaman: *Scripta Mater.*, 1998, vol. 36, pp. 699-705.
11. Y. Liu and D. Favier: *Acta Mater.*, 2000, vol. 48, pp. 3489-99.
12. E. Hornbogen, V. Mertinger, and D. Wurzel: *Scripta Mater.*, 2001, vol. 44, pp. 171-78.
13. Y. Liu and P.G. McCormick: *Mater. Trans. JIM*, 1996, vol. 37, pp. 691-96.
14. D. Mari and D.C. Dunand: *Metall. Mater. Trans. A*, 1995, vol. 26A, pp. 2833-47.
15. L. Bataillard, J.E. Bidaux, and R. Gotthardt: *Phil. Mag. A*, 1998, vol. 78, pp. 327-44.
16. J. Khalil-Allafi, X. Ren, and G. Eggeler: *Acta Mater.*, 2002, vol. 50, pp. 793-803.
17. J.I. Kim, Y. Liu, and S. Miyazaki: *Acta Mater.*, 2004, vol. 52, pp. 487-99.
18. H. Sitepu, W.W. Schmahl, J.K. Allafi, G. Eggeler, A. Dlouhy, D.M. Toebbens, and M. Tovar: *Scripta Mater.*, 2002, vol. 46, pp. 543-48.
19. A. Dloughy, J. Khalil-Allafi, and G. Eggeler: *Phil. Mag.*, 2003, vol. 83, pp. 339-63.
20. D. Chrobak, D. Stroz, and H. Morawiec: *Scripta Mater.*, 2003, vol. 48, pp. 571-76.
21. T. Grosdidier, A.A. Hazotte, and A. Simon: in *High-Temperature Materials for Power Engineering 1990*, E. Bachelet, *et al.*, eds., Kluwer, London, 1990, pp. 1271-80.
22. B. Marty, P. Moretto, P. Gergaud, J.L. Lebrun, K. Ostolaza, and V. Ji: *Acta Mater.*, 1997, vol. 45, pp. 791-800.
23. E. Hornbogen: *Acta Metall.*, 1985, vol. 33, pp. 595-601.
24. E. Hornbogen, V. Mertinger, and D. Wurzel: *Scripta Mater.*, 2001, vol. 44, pp. 171-78.
25. C. Somsen, H. Zahres, J. Kastner, E.F. Wassermann, T. Kakeshita, and T. Saburi: *Mater. Sci. Eng. A*, 1999, vols. A273–A275, pp. 310-14.
26. X. Ren, N. Miura, J. Zhang, K. Ostuka, K. Tanaka, M. Koiwa, T. Suzuki, Y. Chumlyakov, and M. Asai: *Mater. Sci. Eng. A*, 2001, vol. A312, pp. 196-206.